THE JOURNAL OF BIOLOGICAL CHEMISTRY VOL. 285, NO. 4, pp. 2591–2600, January 22, 2010

Phosphorylation of α-Actinin 4 upon Epidermal Growth Factor Exposure Regulates Its Interaction with Actin*

Received for publication, June 19, 2009, and in revised form, November 4, 2009 Published, JBC Papers in Press, November 17, 2009, DOI 10.1074/jbc.M109.035790

Hanshuang Shao, Chuanyue Wu, and Alan Wells[1]

From the Department of Pathology, University of Pittsburgh School of Medicine, Pittsburgh, Pennsylvania 15261

The ubiquitously expressed family of α-actinins bridges actin filaments to stabilize adhesions, a process disrupted during growth factor-induced migration of cells. During the dissolution of the actin cytoskeleton, actinins are phosphorylated on tyrosines, although the consequences of this are unknown. We expressed the two isoforms of human α-actinin in murine fibroblasts that express human epidermal growth factor receptor (EGFR) and found that both α-actinin 1 (ACTN1) and α-actinin 4 (ACTN4) were phosphorylated on tyrosine residues after stimulation with EGF, although ACTN4 was phosphorylated to the greater extent. This required the activation of Src protein-tyrosine kinase and p38-MAPK (and phosphoinositide trisphosphate kinase in part) but not MEK/ERK or Rac1, as determined by inhibitors. The EGF-induced phosphorylation sites of ACTN4 were mapped to tyrosine 4, the major site, and tyrosine 31, the minor one. Truncation mutagenesis showed that the C-terminal domains of ACTN4 (amino acids 300–911), which cross-link the actin binding head domains, act as an inhibitory domain for both actin binding and EGF-mediated phosphorylation. These two properties were mutually exclusive; removal of the C terminus enhanced actin binding of ACTN4 mutants while limiting EGF-induced phosphorylation, and conversely EGF-stimulated phosphorylation of ACTN4 decreased its affinity to actin. Interestingly, a phosphomimetic of tyrosine 265 (which can be found in carcinoma cells and lies near the K255E mutation that causes focal segmental glomerulosclerosis) demonstrated increased actin binding activity and susceptibility of ACTN4 to calpain-mediated cleavage; this variant also retarded cell spreading. Remarkably, either treatment of cells with low concentrations of latrunculin A, which has been shown to depolymerize F-actin, or the deletion of the actin binding domain (100–252 amino acids) of ACTN4Y265E restored EGF-induced phosphorylation. An F-actin binding assay *in vitro* showed that Y4E/Y31E, a mimetic of diphosphorylated ACTN4, bound F-actin slightly compared with wild type (WT). Importantly, the EGF-mediated phosphorylation of ACTN4 at tyrosine 4 and 31 significantly inhibited multinucleation of proliferating NR6WT fibroblasts that overexpress ACTN4. These results suggest that EGF regulates the actin binding activity of ACTN4 by inducing tyrosyl-directed phosphorylation.

Cell motility results from a complex and dynamic process that integrates adhesion and signaling receptors via intracellular signaling cascades at the level of the actin cytoskeleton. To accomplish locomotion, growth factor receptor occupancy leads to phosphorylation cascades that direct cytoskeletal liability and adhesion turnover. This requires actin filaments to be both unbridged and dissociated from the focal adhesions. Because α-actinins are a family of proteins that predominate in cross-linking actin filaments to stabilize transcellular stresses in sessile cells, these proteins have been long thought to be the targets for the signals that drive cell migration.

α-Actinins are a ubiquitously expressed protein family whose isoforms cross-link actin filaments by forming antiparallel homodimers of the extended rod domains (1). To date, at least four human α-actinin genes have been described, with actinin 1 and 4 being ubiquitously expressed in non-muscle cells (2). α-Actinins consist of three conserved domains: an N-terminal actin binding module, a central region composed of four spectrin-like repeats, and a C-terminal calmodulin binding domain (2). Through the N-terminal actin binding domain, α-actinin directly links the actin filaments (3). In addition to bridging the actin filament network, actin-bound actinins drive the actin filaments to focal adhesion sites through the interaction with adhesion plaque proteins talin and vinculin (4).

Adhesion turnover is critical for locomotion of fibroblasts and endothelial and epithelial cells during organogenesis and wound repair (5, 6) and for cancer cells during dissemination (7). Upon growth factor stimulation, the actin cytoskeleton is reorganized from large, bundled filaments to growing networks at the front (8), whereas adhesions disassemble (9); this transition requires the uncoupling of α-actinins from the actin filaments. At the rear of the cell, the actin cytoskeleton dissociates from the adhesion plaques at least in part due to calpain-mediated proteolysis of key bridging molecules (9), including α-actinin (10). Thus, α-actinin regulates cell motility at multiple levels. Furthermore, changes in amino acid charge have been linked to human conditions; a naturally occurring mutation in the dimerization domains (K255E) leads to focal segmental glomerulosclerosis (11), and tyrosine in the same helix 14 (12) was found phosphorylated in human carcinomas (13, 14). Thus, it opens the question of growth factor receptor-mediated phosphorylation of α-actinins regulating their function.

α-Actinin 1 (ACTN1)[2] has been shown to be phosphorylated at tyrosine 12 by focal adhesion kinase (2), with this phosphor-

* This work was supported, in whole or in part, by grants from the National Institutes of Health NIGMS and NIDDK.

[1] To whom correspondence should be addressed: 713 Scaife, Dept. of Pathology, University of Pittsburgh, Pittsburgh, PA 15261. Fax: 412-647-8567; E-mail: wellsa@upmc.edu.

[2] The abbreviations used are: ACTN1, α-actinin 1; ACTN4, α-actinin 4; EGF, epidermal growth factor; EGFR, EGF receptor; GFP, green fluorescent protein; WT, wild type; ERK, extracellular signal-regulated kinase; PBS, phosphate-buffered saline; RIPA, radioimmune precipitation assay buffer; PVDF, polyvinylidene difluoride; MAPK, mitogen-activated protein kinase; MEK, MAPK/ERK kinase.

TABLE 1
ACTN DNA constructs and primers

DNA constructs*	Sense primers	Antisense primers
WT ACTN1 (1–892 aa)	5′-cttcgaattctcatggaccattatgattctcag	5′-ccgcggtaccaggaggtcactctcgccgtacag
WT ACTN4 (1–911 aa)	5′-cttcgaattctcatggtggactaccacgcggcg	5′-ccgcggtaccagcaggtcgctctcgccatacaag
ACTN4 1–230 aa	5′-cttcgaattctcatggtggactaccacgcggcg	5′-ccgcggtaccagcacttcgaaggcattgttcagg
ACTN4 1–260 aa	5′-cttcgaattctcatggtggactaccacgcggcg	5′-ccgcggtaccagataggtcattatggccttctcgtc
ACTN4 1–275 aa	5′-cttcgaattctcatggtggactaccacgcggcg	5′-ccgcggtaccagttcagccttctgcgctcctg
ACTN4 1–300 aa	5′-cttcgaattctcatggtggactaccacgcggcg	5′-ccgcggtaccagcttctctgtagtcctccatcag
ACTN4 300–911 aa	5′-cttcgaattctcctggccagcgacctcctggag	5′-ccgcggtaccagcaggtcgctctcgccatacaag
ACTN4Y4F	5′-cttcgaattctcatggtggac**tt**ccacgcggcgaaccagtcgtac	5′-ccgcggtaccagcaggtcgctctcgccatacaag
ACTN4Y4E	5′-cttcgaattctcatggtggac**gag**cacgcggcgaaccagtcgtac	5′-ccgcggtaccagcaggtcgctctcgccatacaag
ACTN4Y31F	5′-cagcatgggcgac**ttc**atggcccaggagg	
ACTN4Y31E	5′-cagcatgggcgac**gag**atggcccaggagg	
ACTN4Y4E/Y31F	5′-cttcgaattctcatggtggac**ttc**cacgcggcgaaccagtcgtac	5′-ccgcggtaccagcaggtcgctctcgccatacaag
ACTN4Y4E/Y31E	5′-cttcgaattctcatggtggac**gag**cacgcggcgaaccagtcgtac	5′-ccgcggtaccagcaggtcgctctcgccatacaag

Bold letters in sequences indicate mutagenesis sites.
* aa, amino acids.

ylation decreasing the affinity of ACTN1 to actin. However, most non-muscle cells express the two major isoforms of α-actinin and the phosphorylation, and role of α-actinin 4 (ACTN4) remains unclear. In this study, we found that both ACTN1 and ACTN4 were phosphorylated on tyrosines upon cell stimulation by epidermal growth factor (EGF). The phosphorylation sites of ACTN4 were mapped to tyrosine 4 and 31 in the actin binding head domain, with this phosphorylation reducing actin association. Interestingly, the large homodimerizing domain limited the EGF-induced phosphorylation, and removal of the rod domain both enhanced actin binding but also allowed for more efficient phosphorylation. This decrement in F-actin binding allowed for cell behaviors that rely upon rapid actin cytoskeleton remodeling. These findings suggest that ACTN4 phosphorylation downstream of EGF receptor (EGFR) signaling promotes actin filament dissolution.

MATERIALS AND METHODS

Antibodies and Cell Lines—Monoclonal anti-green fluorescent protein (GFP) (catalogue no. A11120) was purchased from Invitrogen. Anti-phosphotyrosine (catalogue no. 9411), anti-phospho-AKT (Ser^{473}) (catalogue no. 9271), and anti-phospho-ERK42/44 (catalogue no. 4377) were purchased from Cell Signaling Technology (Danvers, MA). Anti-vinculin (catalogue no. V9131) and anti-actin (catalogue no. A2668) were purchased from Sigma. NR6WT murine fibroblasts expressing the human EGFR were culture in α-MEM (catalogue no. 15-012-CV; Cellgro, Lawrence KS) with 7.5% fetal bovine serum, 1× nonessential amino acids, 1× sodium pyruvate, 2 mM L-glutamine, 1× streptomycin/penicillin (Invitrogen) supplemented with 350 μg/ml G418 (catalogue no. 345810; EMD, Gibbstown, NJ).

Mutagenesis of ACTN4 and Construction of Expression Plasmid—All site-directed and truncated mutations of ACTN4 were performed by site-directed PCR. After purification and restricted enzyme digestion, WT and mutant actinin DNA fragments were cloned into expression vector pEGFP-N1 to generate GFP fusion proteins. All constructs were confirmed by DNA sequencing. All primers used in plasmids construction and mutagenesis are listed in Table 1.

Expression and Purification of WT ACTN4 and Its Mutants in Escherichia coli—Full-length WT and mutant ACTN4 cDNA sequences were subcloned into bacterial expression vector pET-28a to construct His-tagged proteins; they were transformed into BL21 strain and induced with 1 mM isopropyl 1-thio-β-D-galactopyranoside for 4 h at 37 °C for protein expression. Cells were harvested and then lysed in nickel column-binding buffer in the presence of protease inhibitors mixture set V (catalogue no. 539137; EMD Calbiochem). The purifications of soluble proteins were performed following the manufacturer's introduction of HisTrap™ HP (catalogue no. 17-5247-01; GE Healthcare). Fractions containing target protein were pooled and dialyzed against actin-binding buffer for 24 h at 4 °C with several changes of buffer.

F-actin Filament Sedimentation Assays—F-actin filament sedimentation assays were performed as described previously (11). In brief, recombinant WT or mutant ACTN4 was mixed with 10 μg of G-actin (catalogue no. 3653; Sigma) in reaction buffer containing 10 mM Tris-HCl, pH 7.4, 2 mM $MgCl_2$, 120 mM NaCl, 0.5 mM ATP, and 0.5 mM EGTA for 1 h at room temperature. F-actin filaments were sedimented at 100,000 × *g* for 30 min at 22 °C. Pellets were solubilized in SDS-sample buffer. Equal amounts of proteins from supernatants and pellets separated by 7.5% SDS-PAGE were visualized by Coomassie Blue G-250 staining. Reactions without G-actin were used as a control for nonspecific centrifugation. Band intensities were quantified using ImageJ software (National Institutes of Health).

Binucleated Cell Assay—NR6WT fibroblasts were transiently transfected with eGFP-fused WT or mutant ACTN4 cDNA. After 16 h, media containing transfection reagents were replaced with normal growth media and then incubated for 48 h. Live cells were trypsinized and reseeded in 6-well plates coated with 1 μg/ml fibronectin (catalogue no. F1141; Sigma) for a further 2-h incubation. After a brief wash with PBS, cells were fixed with 2% formaldehyde following by imaging under Olympus fluorescent microscope for analyzing the percent of dual and multinucleated cells.

Cell Spreading Assay—NR6WT fibroblasts transiently transfected with eGFP-fused WT or mutant ACTN4 cDNA were reseeded in 6-well plates coated with 1 μg/ml fibronectin and then incubated for indicated period of time. After incubation, cells were fixed with 2% formaldehyde at room temperature for 30 min and then washed three times with PBS. Images were taken under Olympus fluorescent microscope and the area of transfected cells were measured with ImageJ software.

Immunoprecipitation and Immunoblotting—NR6WT fibroblasts transfected with either WT or mutant ACTN4 were quiesced in α-MEM containing 0.1% dialyzed fetal bovine serum for 6 h and then stimulated with 10 nM EGF for 15 min. Cells were washed briefly with PBS and lysed in RIPA buffer in the presence of protease inhibitors cocktails set V (catalogue no. 539137; EMD Calbiochem). After sonication and centrifugation, the supernatant was incubated with a monoclonal antibody directed against GFP on a shaker at 4 °C overnight after which 20 μl of protein G-Sepharose slurry (catalogue no. 6511-5; Biovision, Mountain View, CA) was added for pull-downs. After washing three times, sample buffer with β-mercaptoethanol was added to the pelleted beads; this was boiled prior to loading on SDS-PAGE. Proteins were transferred to polyvinylidene difluoride (PVDF) membrane and immunoblotted with appropriate primary antibodies according to standard immunoblotting protocols.

m-Calpain Proteolysis Assay—The proteolysis of ACTN4 by m-calpain was performed as described previously (10). Actinin 4-eGFP purified by immunoprecipitation of monoclonal GFP antibody was incubated with 100 ng of m-calpain in proteolysis buffer (20 mM Tris-HCl, pH7.3, 10 mM dithiothreitol, and 1 mM $CaCl_2$) at 30 °C for 30 min. The reaction was stopped by the addition of 5× SDS-sample buffer followed by a 3-min heating in a boiling water bath. Proteins separated by SDS-PAGE were transferred to PDF membrane followed by staining with Coomassie Blue.

Immunostaining—NR6WT fibroblasts grown on coverslips coated with fibronectin were fixed with 2% formaldehyde at room temperature for 30 min. After three washes with PBS (5 min each wash), the cells were permeabilized with 0.1% Triton X-100 diluted in PBS on ice for 5 min and then completely washed with PBS followed by blocking with 1% bovine serum albumin resolved in PBS for 30 min at room temperature. Cells were incubated with various primary antibodies for 1 h at room temperature and then washed three times with PBS (10 min each wash). Subsequently, rhodamine phalloidin (1:500 final dilution in PBS) was added and incubated for 45 min at room temperature. The cells were washed three times (10 min each wash). The coverslips were then transferred inversely to a glass slide carrying a drop of Mowiol 4-88 (catalogue no. 81381; Sigma) and digitally photographed (Olympus).

RESULTS

EGF Stimulates the Phosphorylation of α-ACTN4 on Tyrosines—Growth factors stimulate chemokinesis, at least in part, by altering the linkages between the cytoskeleton and the membrane adhesion sites (6, 15); this includes dissolution of focal complexes and loss of central actin cables (9). Because α-actinins serve to bridge individual actin filaments, we asked whether α-actinin localization or function may be altered upon EGFR activation. We acutely exposed to EGF (10 nM for 10 min) murine fibroblast NR6WT cells expressing GFP-tagged α-actinin isoforms (Fig. 1*A*). Because antibodies specific for individual tyrosyl-phosphorylated actinin are not available, we pulled down GFP-tagged actinins by immunoprecipitation using monoclonal GFP antibody and then immunoblotted against phosphotyrosine. We found that both ACTN1 and ACTN4 were tyrosyl-phosphorylated with ACTN4 being labeled more strongly (Fig. 1*B*). Vanadate has been shown to enhance the phosphorylation of ACTN1 by blocking the activity of phosphatase 1B (2). As shown in Fig. 1*C*, NR6WT treated with 300 μM vanadate for 30 min prior to the addition of EGF significantly enhanced the phosphorylation of both ACTN1 and ACTN4. Because ACTN4 has been implicated in adhesive processes (16), we pursued this isoform.

Although it is quite possible that the tyrosyl phosphorylation is direct via the EGFR (or indirect via activation of focal adhesion kinase, which has been shown to phosphorylate ACTN1) (2), coordinate required signaling pathways were probed (Fig. 1*D*). Inhibition of EGFR by a small molecule tyrosine kinase inhibitor blocked this phosphorylation as expected, although surprisingly so did the p38 inhibitor SB203580; the phosphoinositide trisphosphate kinase inhibitor LY294002 reduced phosphorylation by about one-third (Fig. 1, *D* and *E*). To determine the p38-related signaling pathway involved in EGF-mediated phosphorylation of ACTN4, cells transfected with WT ACTN4 were incubated with the Src tyrosine kinase inhibitor PP2 or Rac1 inhibitor prior to the addition of EGF. As shown in Fig. 1*F*, PP2, but not Rac1 inhibitor, completely blocked the phosphorylation of ACTN4 through the inhibition of phosphorylation of p38 at Thr^{180}/Tyr^{182}. Interestingly, blocking the robust MEK/ERK MAP kinase pathway had no discernable effect on tyrosyl phosphorylation of both ACTN1 and ACTN4. These results suggested that the p38 signal pathway is involved in the phosphorylation of ACTN1 and ACTN4 stimulated by EGF. However, because p38 is not a tyrosine kinase, this suggests an indirect effect of this pathway on ACTN4 phosphorylation, the dissection of which lies beyond the scope of the present article.

Tyrosines 4 and 31 are the Main EGF-mediated Phosphorylation Sites of ACTN4—Murine ACTN4 has been shown to be phosphorylated at tyrosine 266 (corresponding to tyrosine 265 in the human sequence) in NIH 3T3 cells expressing constitutively active c-Src (Y527E tyrosine kinase) by the use of reversed phase liquid chromatography-tandem mass spectrometry (13), and human ACTN4 has also been reported to be phosphorylated at tyrosine 265 as determined using a phosphoproteomic approach (14). To determine whether tyrosine 265 of human α-ACTN4 is also the site phosphorylated upon EGF stimulation, we replaced the tyrosine 265 by phenylalanine to abolish phosphorylation or by glutamic acid to mimic the phosphorylated protein. To our surprise, the mutant ACTN4Y265F was still phosphorylated by EGF at the same level as WT ACTN4 (Fig. 2*A*, *lanes 1–4* and *7–10* for truncated fragment-(1–400)). Interestingly, the mutant ACTN4Y265E with enhanced actin binding activity was not phosphorylated in response to EGF (Fig. 2*A*, *lanes 5* and *6*, and *11* and *12* for truncated fragment-(1–400)); this finding is probed in subsequent experiments (see below).

To identify the phosphorylation site of ACTN4 further, we first divided ACTN4 into an N-terminal fragment-(1–300) (the actin binding "head" group) and a C-terminal fragment-(300–911) (the rod and calmodulin binding domains) based on structural domains (2). As shown in Fig. 2*B*, the phosphorylation site resides within fragment-(1–300). Because there were 10

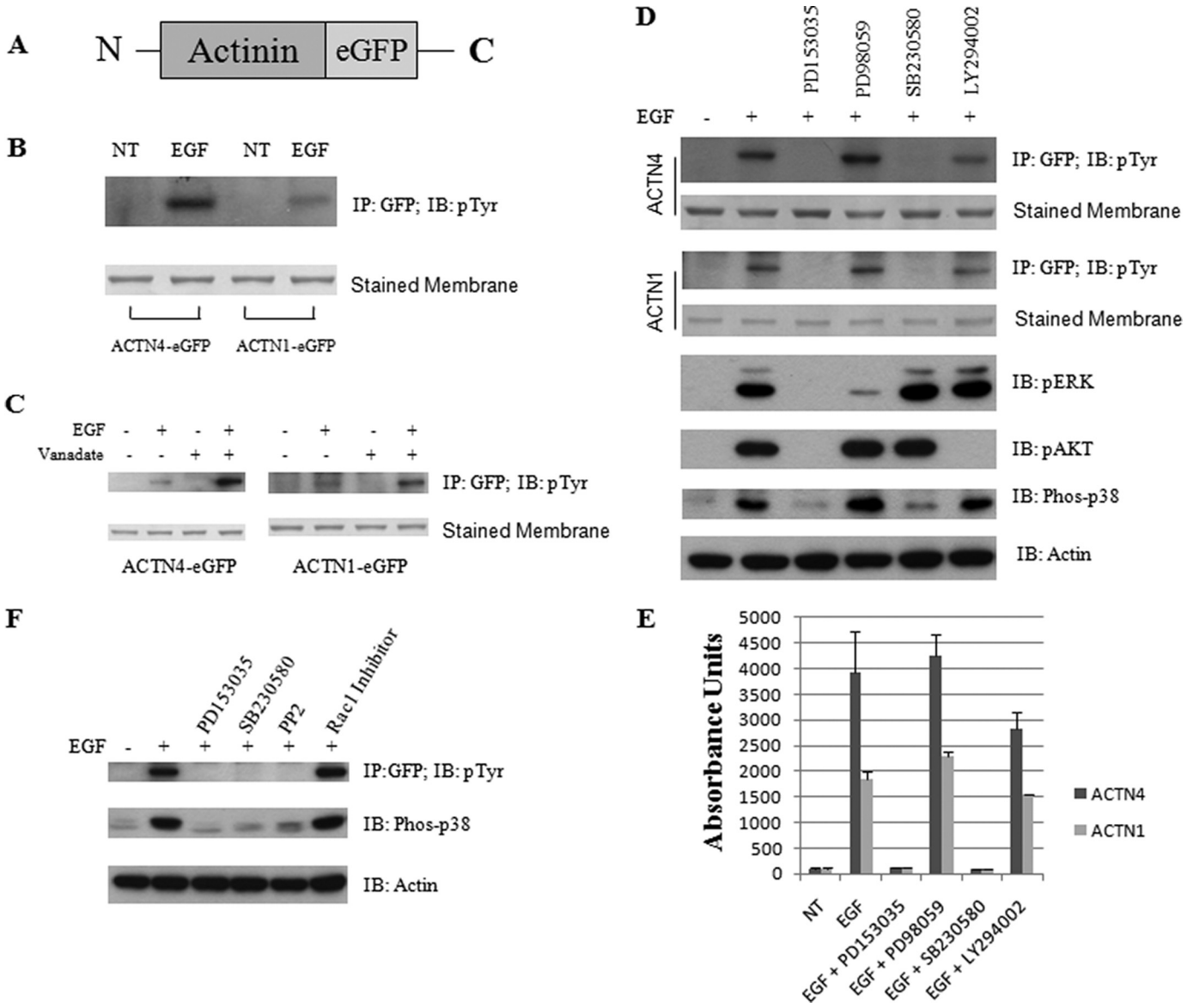

FIGURE 1. **EGF stimulated the phosphorylation of ACTN through the p38-MAPK signaling pathway.** *A*, diagram of full-length ACTN tagged by EGFP at the C terminus is shown. *B*, NR6WT fibroblasts expressing ACTN1-eGFP or ACTN4-eGFP were quiesced with quiescence media containing 0.1% dialyzed fetal bovine serum for 6 h prior to an addition of 10 nM EGF. After EGF stimulation for 10 min, cells were washed once with cold PBS and then lysed with RIPA buffer containing 1× protease inhibitors mixture. ACTN1-eGFP and ACTN4-eGFP were purified by immunoprecipitation (*IP*) against monoclonal GFP antibody and separated by SDS-PAGE and then immunoblotted (*IB*) with α-phosphotyrosine (*pTyr*) antibody (*upper panel*). Total protein transferred to PVDF membrane was stained with Coomassie Blue G-250 (*lower panel*). *NT*, no treatment. *C*, vanadate (300 μM) pretreatment enhanced the phosphorylation of both ACTN1 and ACTN4. *D*, NR6WT fibroblasts expressing WT ACTN1-eGFP or ACTN4-eGFP were pretreated with different 10 μM inhibitors for 30 min prior to EGF stimulation. Cells were lysed with RIPA buffer, and equal amounts of total protein were loaded for SDS-PAGE and then immunoblotted as shown. The control panels demonstrating agent-specific inhibition are from the ACTN4-eGFP cells, but identical results were obtained in the ACTN1-eGFP cells. *E*, phosphorylation level of both ACTN4 and ACTN1 in all treatments was quantitated using software ImageJ. *F*, NR6WT fibroblasts expressing WT ACTN4-eGFP were pretreated with 10 μM protein-tyrosine kinase inhibitor PP2 or Rac1 inhibitor for 30 min prior to EGF stimulation. ACTN4-eGFP was purified by immunoprecipitation against monoclonal GFP antibody, and cells were lysed with RIPA buffer. Equal amounts of either purified ACTN4-eGFP or total protein were separated by SDS-PAGE and then were immunoblotted as shown. Shown are representative immunoblots of at least three for each experiment. *Error bars* indicate ±S.D.

tyrosines within fragment-(1–300), we individually replaced all 10 N-terminal tyrosines of full-length ACTN4 with phenylalanine (data not shown) and found that the tyrosine 4 was the major phosphorylation site and the tyrosine 31 was a minor one (Fig. 2*C*). Interestingly, phosphorylation of the truncated fragment-(1–400) (Fig. 2*A*, *lanes 7* and *8*) and fragment-(1–300) (Fig. 2*D*) was much stronger than full-length WT ACTN4, indicating that the C terminus may act as an inhibitory domain for phosphorylation.

ACTN4Y265E Mutant Has Abnormal Cellular Localization and Enhanced Susceptibility to Cleavage by m-Calpain—The crystal structure of the actin binding domain of the ACTN4K255E mutant resolved by Dominguez's group showed that the tyrosine 265 was localized within the helix 14 (12) and that this pathologically occurring mutation enhanced actin binding activity with abnormal colocalization with actin (11). Because the nearby tyrosine at amino acid 265 is reported to be phosphorylated (13, 14), we replaced tyrosine 265 with gluta-

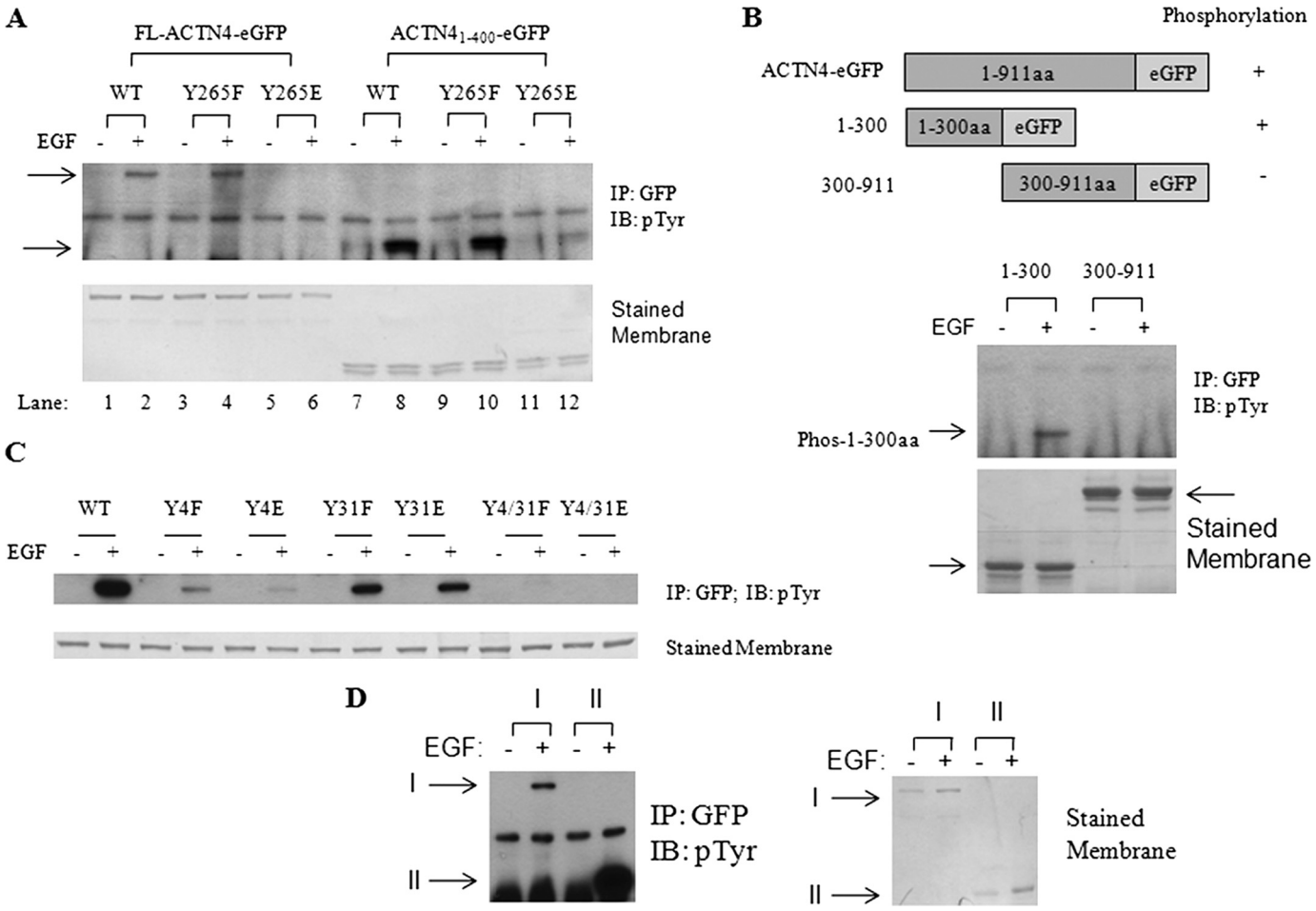

FIGURE 2. **Identification of the phosphorylation sites of ACTN4.** *A*, NR6WT fibroblasts transfected with full-length or truncated WT ACTN4-eGFP or Y265F and Y265E mutants were quiesced and then stimulated with 10 nM EGF for 10 min prior to immunoprecipitation (*IP*) of GFP antibody. Membrane was immunoblotted (*IB*) against phosphotyrosine (*pTyr*; *upper panel*) and stained with Coomassie Blue G-250 (*lower panel*). *B*, diagram of ACTN4 truncated mutants tagged with eGFP is shown (*left*). Protein was purified by GFP immunoprecipitation and then immunoblotted against pTyr antibody (*right upper panel*) and stained with Coomassie Blue G-250 (*right lower panel*). *C* and *D*, WT and mutant ACTN4-eGFP purified by GFP immunoprecipitation were immunoblotted against phosphotyrosine antibody (*upper panels*), and the membrane was stained with Coomassie Blue G-250 (*lower panels*). *Arrows* indicate the target proteins. Shown are representative immunoblots of at least three for each experiment. *I*, WT-ACTN4-eGFP; *II*, ACTN4-1-300-eGFP.

minic acid as a phosphomimetic to examine the consequences of the previously defined phosphorylations on ACTN4. We found that the cellular localization of ACTN4Y265E was altered in comparison with WT ACTN4 by either being retained at the rear of locomoting cells (Fig. 3*A*) or accumulating at the peripheral membrane (data not shown). ACTN4Y265F had cellular localization similar to WT ACTN4 (Fig. 3*A*). The cellular localization of ACTN4Y265E, which strongly binds F-actin (Fig. 3*C*), appeared similar to the reported localization of kidney disease-associated ACTN4 mutant K255E in podocytes (11, 16).

ACTN1 has been shown to be a substrate of m-calpain (17, 18), with the cleavage site localized between tyrosine 246 (for ACTN1) or 265 (for ACTN4) and the subsequent histidine (10). This would remove the actin binding from the cross-linking activities. However, how the calpain susceptibility is regulated remains unknown. We incubated immunopurified WT ACTN4, ACTN4Y265F, and ACTN4Y265E with 100 ng of pure recombinant m-calpain at 30 °C for 30 min followed by SDS-PAGE. As shown in Fig. 3*B*, m-calpain cleaved about half of the WT ACTN4 and ACTN4265F within 30 min of incubation. Interestingly, the ACTN4Y265E mutant was completely digested by m-calpain, suggesting that phosphorylation of tyrosine 265 significantly exposes the cleavage site to m-calpain. Because m-calpain is activated by growth factors (5, 19), this suggests that there may be a dual control of actin cross-linking with Src family kinase phosphorylating tyrosine 265 to make this molecule accessible to calpain-mediated separation of the actin binding and actin cross-linking domains. Furthermore, expression of the strongly actin-binding Y265E significantly delayed the spreading of NR6WT fibroblasts compared with WT ACTN4 and Y265F (Fig. 3*D*). This suggests that the enhanced F-actin binding capability limits the cytoskeletal plasticity needed for spreading. Taken together, these data implied that tyrosine 265 is a key residue in maintaining the integrity of ACTN4 and thus stress fibers.

Binding of ACTN4 to Actin Inhibits Its Phosphorylation—α-Actinin has been suggested to interact with actin filaments through an actinin homodimer that is formed by the antiparallel interaction of four spectin-like repeats. To determine whether the actin binding activity interacts with phosphorylation of ACTN4 by EGF, we constructed two small fragments-

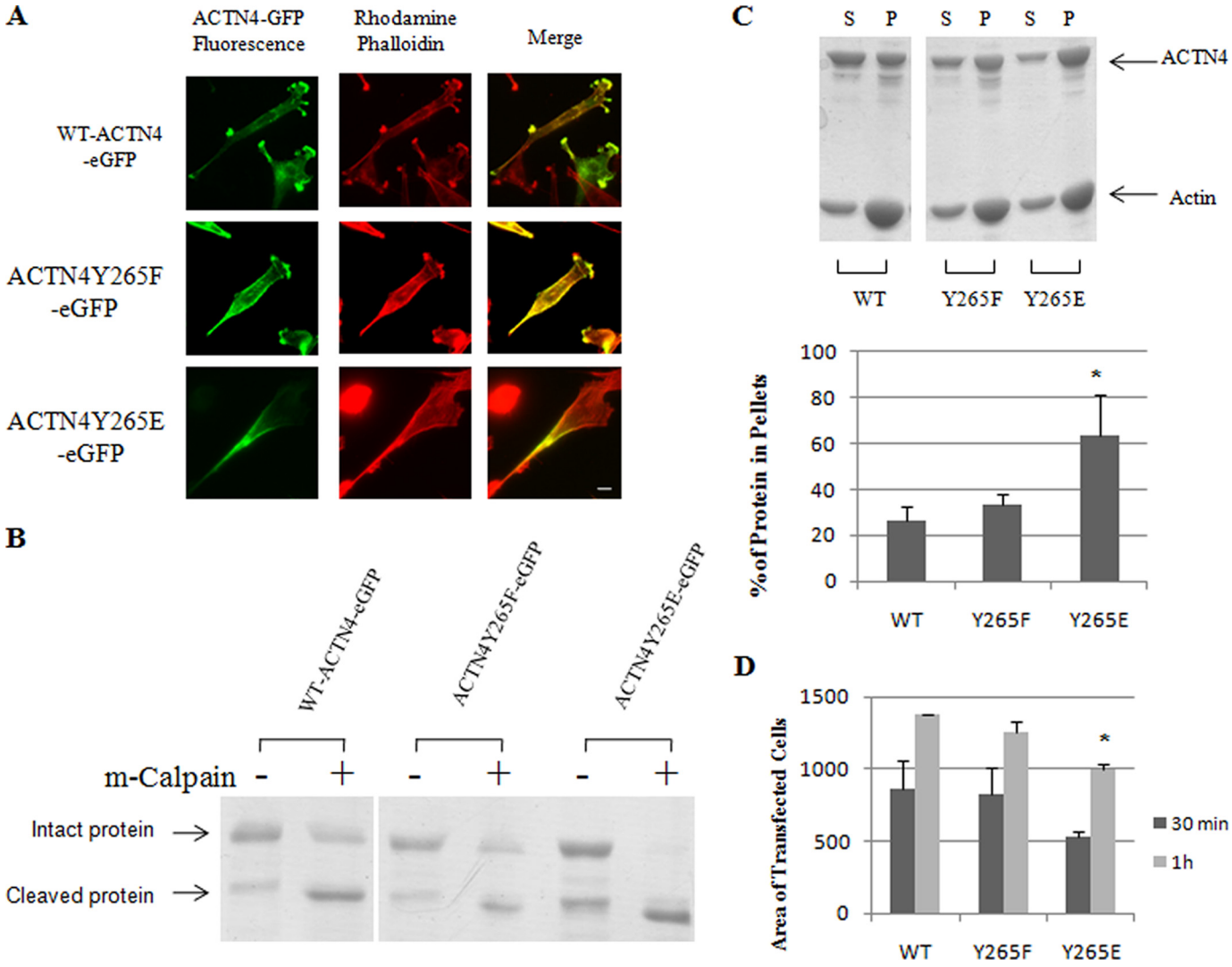

FIGURE 3. **Replacement of ACTN4 tyrosine 265 with glutamine increased F-actin binding activity.** *A*, NR6WT fibroblasts expressing WT or mutant ACTN4-eGFP were fixed and then stained with rhodamine phalloidin. *Scale bar*, 5 μm. *B*, WT and mutant ACTN4-eGFP purified with GFP immunoprecipitation were incubated with 100 ng of pure recombinant m-calpain at 30 °C for 30 min followed by SDS-PAGE. Protein transferred to PVDF membrane was stained with Coomassie Blue G-250. *C*, representative image and quantitative result of Coomassie Blue G-250-stained polyacrylamide gel are shown. F-actin and bound ACTN4 were pulled down by centrifugation at 100,000 $\times$ *g* for 30 min at 25 °C. Equal amounts of supernatant (*S*) and pellets (*P*) were loaded, and reaction without addition of G-actin was considered as a centrifugation control. *, $p < 0.05$, Student's *t* test comparing Y265E with either WT or Y265F. *D*, NR6WT cells transfected with ACTN4-eGFP were reseeded on 6-well plates coated with 1 μg/ml fibronectin and cultured for either 30 min or 1 h prior to fixation. The areas of at least 50 fluorescent cells were measured using ImageJ software. *, $p < 0.05$, Student's *t* test comparing Y265E with either WT or Y265F. Shown are representative results of at least three for each experiment in *A–C*. *Error bars* in *C* and *D* indicate ±S.D.

(1–230) and -(1–260) that contained both the actin binding domain and phosphorylation sites tyrosine 4 and 31, but without the four spectin-like repeats and calmodulin binding motif. When expressed in cells, fragments-(1–230) and -(1–260), which bind to actin very strongly and peripherally aggregate in cells, were not phosphorylated by EGF (Fig. 4, *A* and *B*). Actin was strongly coimmunoprecipitated with both fragments even in the absence of the homodimer domains (Fig. 4*A*), suggesting that the C terminus of ACTN4 is also an inhibitory domain limiting actin binding activity and that this enhanced actin binding activity of the isolated ACTN4 N-terminal domains may prevent access of the phosphorylating kinase. The minimum length of ACTN4 for EGF-mediated phosphorylation and cellular solubility is residues 1–275 (data not shown). To determine further whether binding of ACTN4 to actin filaments affects EGF-induced phosphorylation, NR6WT fibroblasts expressing WT ACTN4-eGFP or ACTN4Y265E-eGFP were treated with low concentration of latrunculin A for 30 min prior to the addition of EGF to depolymerize the actin cytoskeleton. As shown in Fig. 4*D*, latrunculin A treatment of cells restored EGF-induced phosphorylation of ACTN4Y265E at the same time as it eliminated actin binding activity. Together, these findings strongly suggested that the binding of ACTN4 to actin filaments inhibits EGF-mediated phosphorylation.

EGF-stimulated Phosphorylation Decreases the Actin Binding Activity of α-Actinin 4—Based on these findings, we speculated that phosphorylation of ACTN4 would reciprocally lessen binding to actin. To test this, we expressed and purified soluble WT and mutant full-length ACTN4 tagged with polyhistidine at their C termini from bacteria BL21 for actin filament sedimentation assay. As shown in Fig. 5*A*, ACTN4Y4E/Y31E, a dually phosphorylated mimetic pro-

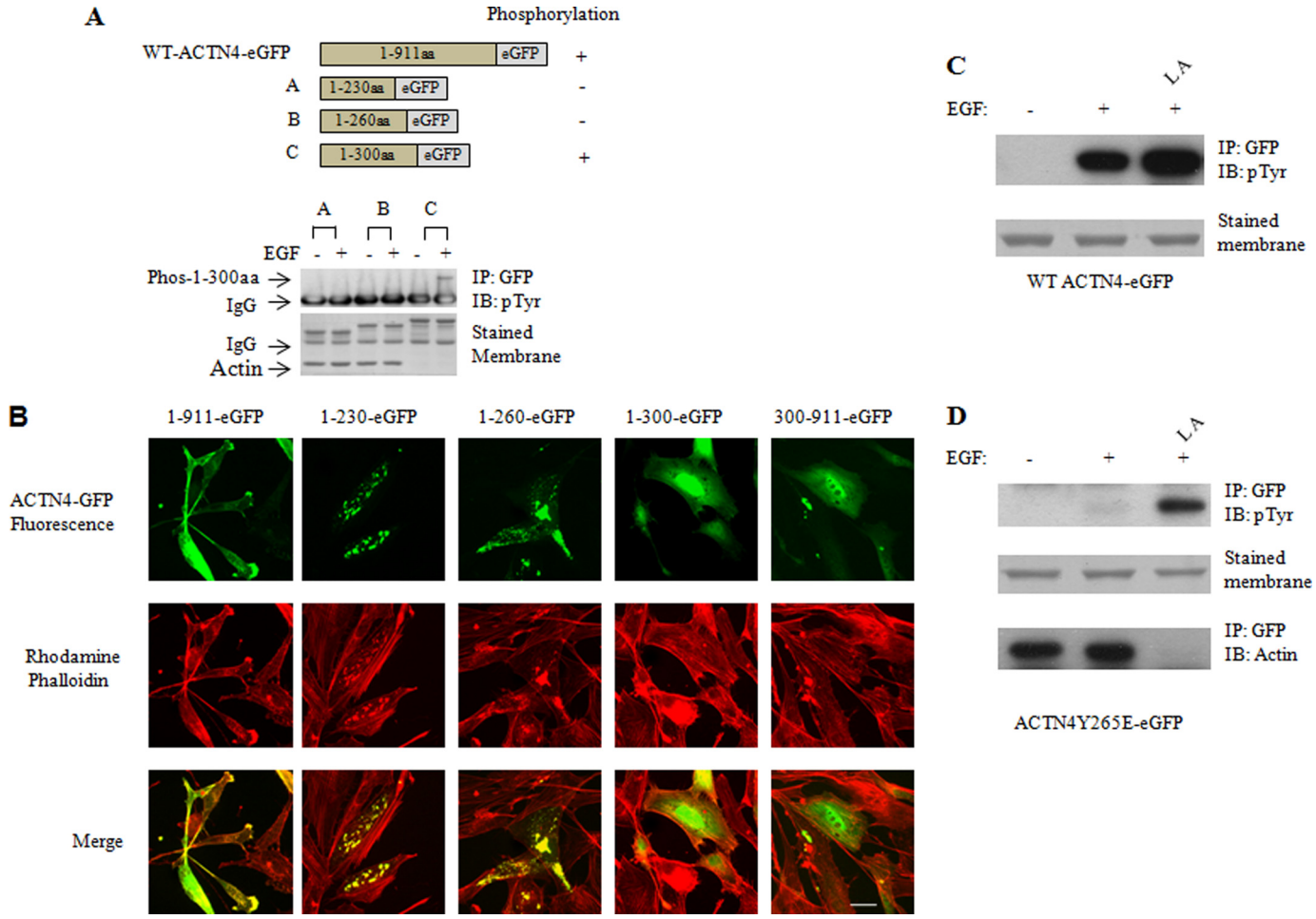

FIGURE 4. **Binding of ACTN4 to actin inhibited EGF-stimulated phosphorylation.** *A*, diagram of truncated ACTN4 mutants tagged with eGFP is shown. Mutants were transfected into NR6WT fibroblasts. Cells quiesced with quiescence media were treated with 10 nM EGF for 10 min. Mutants purified with GFP immunoprecipitation (*IP*) were separated by SDS-PAGE followed by immunoblotting (*IB*) of phosphotyrosine. *B*, NR6WT fibroblasts expressing WT or truncated ACTN4-eGFP were fixed and then immunostained by rhodamine phalloidin. *Scale bar*, 5 μm. *C* and *D*, cells transfected with either WT ACTN4-eGFP or mutant Y265E-eGFP were quiesced and then were pretreated with 300 μM vanadate and 1 μM latrunculin A (*LA*) for 30 min prior to 10 nM EGF for additional 10 min. Interested proteins purified with GFP immunoprecipitation were separated by SDS-PAGE followed by immunoblotting of phosphotyrosine (*pTyr*). Shown are representative immunoblots of at least three for each experiment.

tein, was rarely present in pellet (only 1.1% protein bound to actin filaments), whereas WT was 27.9%. This result suggested that EGF-induced phosphorylation of ACTN4 decreased the actin binding activity.

In an attempt to discern whether actin binding and tyrosyl phosphorylation were mutually exclusive or competitive, we generated an $ACTN4_{\Delta 100-252}$ mutant that lacked the putative actin binding domain based on mapping in ACTN1 (residues 100–252, a region wider than the putative actin binding domain (residues 108–189)) (Fig. 5*B*) (20). In line with this previous report (20), both WT ACTN4 and ACTN4Y265E no longer bound actin filament (Fig. 5*C*). To our surprise, $ACTN4_{\Delta 100-252}$ was still phosphorylated by EGF at a level similar with WT ACTN4 (Fig. 5*D*, *lanes 1* and *3*). More interestingly, $ACTN4_{\Delta 100-252}$ no longer colocalized with rhodamine phalloidin-staining actin in the protrusive leading front of migrating cells (Fig. 5*E*). Thus, the region of residues 100–252 appears to be an essential domain for the colocalization with actin filaments in the leading area of a moving cell, probably through the interaction with other molecules. Furthermore, the ACTN4Y265E mutant that bound actin very tightly was not phosphorylated by EGF stimulation (Fig. 2*A*, *lanes 5* and *6*, and Fig. 5*D*, *lanes 5* and *6*), but the deletion of region 100–252 rescued the EGF-mediated phosphorylation (Fig. 5*D*, *lanes 7* and *8*). These data suggested that the phosphorylation of ACTN4 stimulated by EGF is mutually exclusive with actin binding.

Multinucleation of Cells Is Reduced in Cells with ACTN4 Phosphomimetics—ACTN4 has been shown to be required for tightly regulated remodeling of the actin cortical network during cytokinesis, and >25% of normal rat kidney cells that overexpressed WT ACTN4 were multinucleated because of an increase in equatorial actin filaments (21). To determine whether the EGF-mediated phosphorylation of ACTN4 affects cytokinesis, NR6WT fibroblasts transfected to express either WT ACTN4-eGFP or Y4E/Y31E-eGFP were incubated for a further 48 h. As shown in Fig. 6, many fewer cells transfected with Y4E/Y31E were multinucleated compared with those transfected with WT ACTN4-eGFP. These data suggest that EGF-mediated phosphorylation of ACTN4 decreased actin binding activity and thus down-regulated multinucleation during cytokinesis.

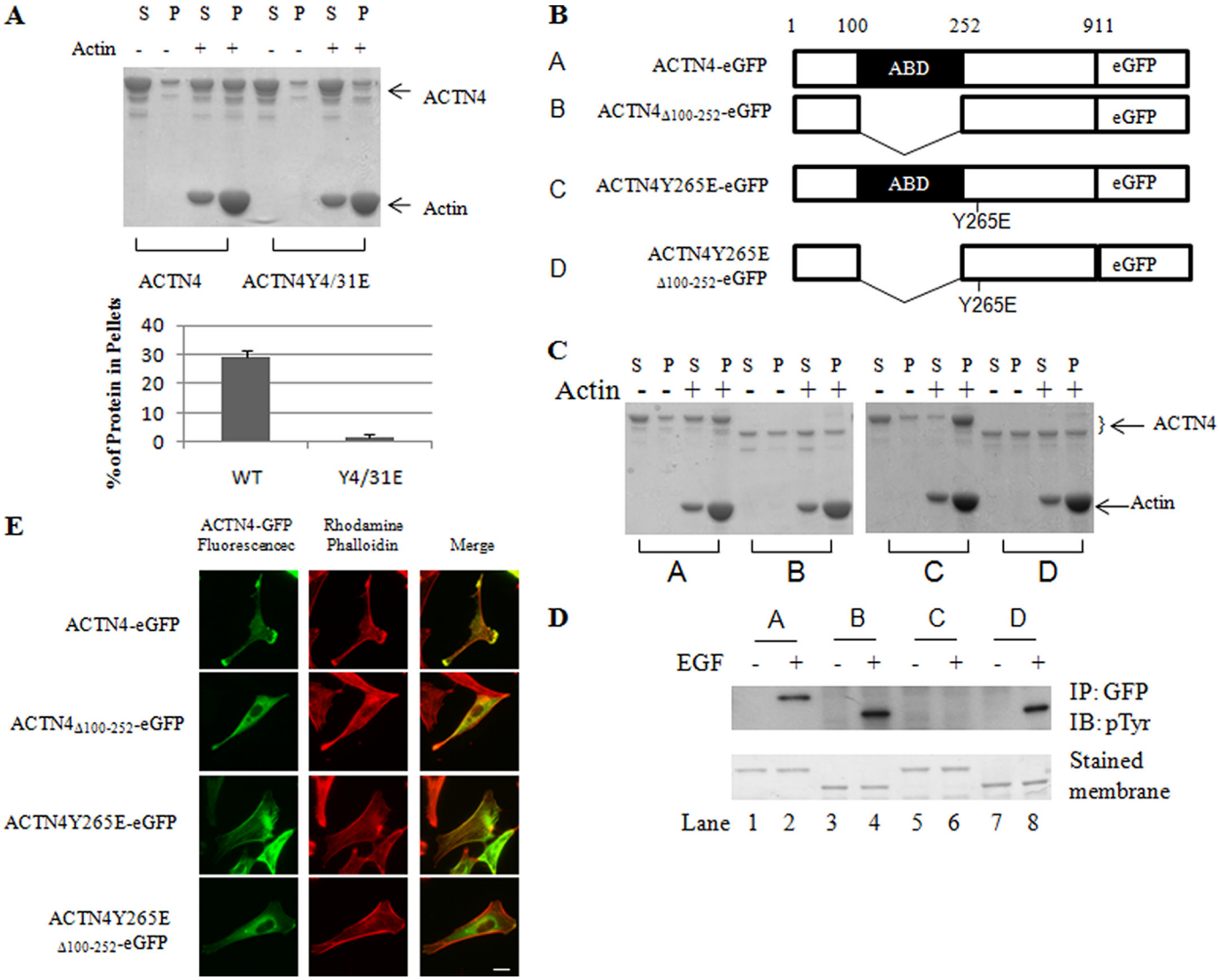

FIGURE 5. **EGF-stimulated phosphorylation of ACTN4 decreased the actin binding activity.** *A* and *C*, representative images and quantitative result of Coomassie Blue G-250-stained polyacrylamide gel. F-actin and bound ACTN4 were pulled down by centrifugation at 100,000 × *g* for 30 min at 25 °C. Equal amounts of supernatant (*S*) and pellets (*P*) were loaded, and reaction without the addition of G-actin was considered as a centrifugation control. Image analysis and quantitation of three experiments are shown for *A*, with $p < 0.01$ between the Y4E/Y31E and WT variants. *Error bars* indicate ±S.D. *B*, diagram of WT and mutant ACTN4-eGFP. *D*, WT or ACTN4 mutants transfected into NR6WT fibroblasts. Cells quiesced with quiescence medium were treated with 10 nM EGF for 10 min. Mutants purified with GFP immunoprecipitation (*IP*) were separated by SDS-PAGE followed by immunoblotting (*IB*) of phosphotyrosine. PVDF membrane containing protein was stained with Coomassie Blue G-250. *E*, NR6WT fibroblasts expressing WT or mutant ACTN4-eGFP fixed and then immunostained by rhodamine phalloidin. *Scale bar*, 5 μm. Shown are representative immunoblots of at least three for each experiment.

DISCUSSION

During induced fast cell motility, the actin cytoskeleton must undergo dramatic change with the disassembly of actin bundles. Because α-actinins play a major role in linking filaments together into strong cables, the regulation of their functioning has been probed. Two isoforms are ubiquitous in non-muscle adherent cells that undergo growth factor-induced migration during repair and tumor invasion. However, the relative contributions and convergence or divergence thereof have not been defined. Thus, this study was undertaken.

ACTN1 has been shown to be phosphorylated at tyrosine 12 by focal adhesion kinase, with the mimetic Y12E mutant having low affinity to actin compared with WT ACTN1 and Y12F (2). Phosphorylated ACTN1 and protein-tyrosine phosphatase 1B coregulated the interaction of focal adhesion kinase and Src and promoted the cell migration (22). To determine the applicability to growth factor-induced motility, we utilized the ubiquitous motogen, EGF. To our surprise, EGF strongly stimulated the phosphorylation of ACTN4, but only weaker phosphorylation of ACTN1. This may be due to the different amino acids at their N termini. Homology analysis of the amino acids of human ACTN1 and ACTN4 revealed that tyrosine 12 of ACTN1 is identical to tyrosine 31 of ACTN4, which we now show to be a minor phosphorylation site for EGF exposure. ACTN4 has an additional 19 amino acids at the N terminus with the other tyrosines within the C terminus being shared. Thus, it was interesting to note that the major site of ACTN4 is precisely this "novel" tyrosine 4. Whether ACTN4 is also phosphorylated by focal adhesion kinase at tyrosine 31 or other tyrosines remains unclear.

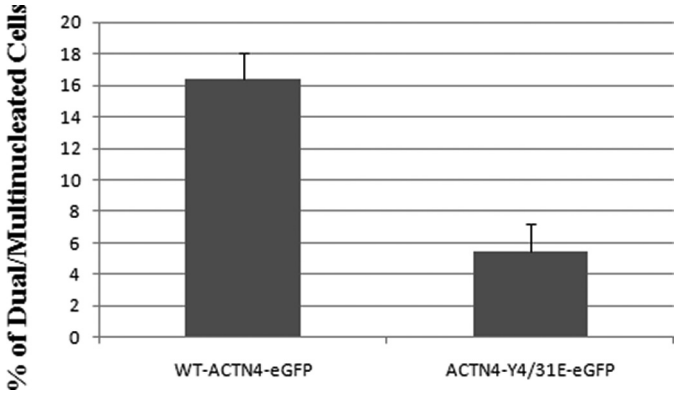

FIGURE 6. **ACTN4 drives multinucleation in NR6WT fibroblasts which is limited by phosphomimetic ACTN4.** NR6WT fibroblasts were transfected with WT ACTN4-eGFP or Y4E/Y31E-eGFP followed by 48-h culture with complete growth media. After trypsinization, cells were reseeded on 6-well plates coated with 1 μg/ml fibronectin and then cultured for an additional 2 h prior to fixation. Percentages of dual/multinucleated cells were analyzed ($n > 200$). $p < 0.01$ comparing cells expressing the WT ACTN4 with those expressing the dual phosphomimetic ACTN4. *Error bars* indicate ±S.D.

Functionally, the two isoforms may be regulated similarly, although the target amino acids may differ. We found that EGF down-regulated the actin binding activity of ACTN4 through the phosphorylation at tyrosine 4 and 31. Once the ACTN4 bound to actin filaments were phosphorylated by EGF stimulation, they disassociated from actin filaments. The nonphosphorylated ACTN4 bound tightly to the actin filaments. Thus, it appears that actin association is determined by the tyrosyl phosphorylation at the N-terminal head of the actin association domain. This model fits well with the finding that EGF leads to actin cable dissolution (9). Tension is required for the formation of focal adhesions (6). A recent study found that α-actinin and actin orchestrate the assembly and maturation of the nascent adhesion (23), implying a targeting sequence. We constructed an ACTN4 mutant lacking the ACTN1-defined actin binding domain residues region 100–252 (named $ACTN4_{\Delta 100-252}$); this protein mutant failed to localize within the protrusive leading area of a moving cell concomitant with its loss of actin binding activity. This suggests that actin-ACTN4 colocalization at the leading edge requires a distinct targeting domain. Murine and human ACTN4 have been shown to be phosphorylated at tyrosine 266 (murine)/265 (human) (13, 14). However, there is no direct biochemical evidence to show that ACTN4 is phosphorylated at this tyrosine upon stimulation by EGF. In this study, we found that EGF did stimulate the phosphorylation of human ACTN4 at tyrosines 4 and 31, but not tyrosine 265 (equal to murine ACTN4 tyrosine 266). Although the tyrosine 265 of human ACTN4 is not the phosphorylation site for EGF exposure, we created a variant ACTN4Y265E to mimic phosphorylated ACTN4; this variant bound actin very tightly and caused an abnormal cellular localization compared with WT ACTN4. This is in line with a human pathology-defined ACTN4 mutant K255E, which has been shown to cause an autosomal dominant of kidney failure (16). Because both lysine 255 and tyrosine 265 resided in the helix 14 of the three-dimensional structure of the N terminus of ACTN4, either lysine 255 or tyrosine 265 replaced with glutamic acid probably significantly altered the confirmation of ACTN4 by exposing the actin binding domain. This property was further confirmed by F-actin sedimentation assay *in vitro* (Fig. 3*C*) and cell spreading assay (Fig. 3*D*). Of interest, the conformational change exposes an m-calpain cleavage site in a manner not dissimilar from phosphoinositide-promoted ACTN1 cleavage (10). This would lead to a nonreversible actin cable dissolution.

Although these and other studies into α-actinin filament cross-linking are still nascent, the findings herein demonstrate the complexity of the α-actinin system. The isoforms, despite being very similar at the sequence level, are quantitatively and qualitatively differentially regulated by growth factors, with distinct functional consequences of even conserved domains. Initial studies (data not shown) that lie beyond the scope of the present article suggest a functional consequence of EGF-induced ACTN4 phosphorylation, in terms of cell motility, although these results are confounded by both isoform redundancy and the multipotent effects of actin cable formation and stabilization.

Acknowledgment—We thank Dr. Yizeng Tu for technical assistance.

REFERENCES

1. Ylänne, J., Scheffzek, K., Young, P., and Saraste, M. (2001) *Structure* **9,** 597–604
2. Izaguirre, G., Aguirre, L., Hu, Y. P., Lee, H. Y., Schlaepfer, D. D., Aneskievich, B. J., and Haimovich, B. (2001) *J. Biol. Chem.* **276,** 28676–28685
3. Fraley, T. S., Pereira, C. B., Tran, T. C., Singleton, C., and Greenwood, J. A. (2005) *J. Biol. Chem.* **280,** 15479–15482
4. Otey, C. A., and Carpen, O. (2004) *Cell Motil. Cytoskeleton* **58,** 104–111
5. Glading, A., Lauffenburger, D. A., and Wells, A. (2002) *Trends Cell Biol.* **12,** 46–54
6. Ridley, A. J., Schwartz, M. A., Burridge, K., Firtel, R. A., Ginsberg, M. H., Borisy, G., Parsons, J. T., and Horwitz, A. R. (2003) *Science* **302,** 1704–1709
7. Wells, A. (2000) *Adv. Cancer Res.* **78,** 31–101
8. Chou, J., Burke, N. A., Iwabu, A., Watkins, S. C., and Wells, A. (2003) *Exp. Cell Res.* **287,** 47–56
9. Xie, H., Pallero, M. A., Gupta, K., Chang, P., Ware, M. F., Witke, W., Kwiatkowski, D. J., Lauffenburger, D. A., Murphy-Ullrich, J. E., and Wells, A. (1998) *J. Cell Sci.* **111,** 615–624
10. Sprague, C. R., Fraley, T. S., Jang, H. S., Lal, S., and Greenwood, J. A. (2008) *J. Biol. Chem.* **283,** 9217–9223
11. Weins, A., Schlondorff, J. S., Nakamura, F., Denker, B. M., Hartwig, J. H., Stossel, T. P., and Pollak, M. R. (2007) *Proc. Natl. Acad. Sci. U.S.A.* **104,** 16080–16085
12. Lee, S. H., Weins, A., Hayes, D. B., Pollak, M. R., and Dominguez, R. (2008) *J. Mol. Biol.* **376,** 317–324
13. Rush, J., Moritz, A., Lee, K. A., Guo, A., Goss, V. L., Spek, E. J., Zhang, H., Zha, X. M., Polakiewicz, R. D., and Comb, M. J. (2005) *Nat. Biotechnol.* **23,** 94–101
14. Rikova, K., Guo, A., Zeng, Q., Possemato, A., Yu, J., Haack, H., Nardone, J., Lee, K., Reeves, C., Li, Y., Hu, Y., Tan, Z., Stokes, M., Sullivan, L., Mitchell, J., Wetzel, R., Macneill, J., Ren, J. M., Yuan, J., Bakalarski, C. E., Villen, J., Kornhauser, J. M., Smith, B., Li, D., Zhou, X., Gygi, S. P., Gu, T. L., Polakiewicz, R. D., Rush, J., and Comb, M. J. (2007) *Cell* **131,** 1190–1203
15. Wells, A., Huttenlocher, A., and Lauffenburger, D. A. (2005) *Int. Rev. Cytol.* **245,** 1–16
16. Dandapani, S. V., Sugimoto, H., Matthews, B. D., Kolb, R. J., Sinha, S., Gerszten, R. E., Zhou, J., Ingber, D. E., Kalluri, R., and Pollak, M. R. (2007) *J. Biol. Chem.* **282,** 467–477
17. Selliah, N., Brooks, W. H., and Roszman, T. L. (1996) *J. Immunol.* **156,** 3215–3221

18. Beckerle, M. C., Burridge, K., DeMartino, G. N., and Croall, D. E. (1987) *Cell* **51,** 569–577
19. Glading, A., Chang, P., Lauffenburger, D. A., and Wells, A. (2000) *J. Biol. Chem.* **275,** 2390–2398
20. Hemmings, L., Kuhlman, P. A., and Critchley, D. R. (1992) *J. Cell Biol.* **116,** 1369–1380
21. Mukhina, S., Wang, Y. L., and Murata-Hori, M. (2007) *Dev. Cell* **13,** 554–565
22. Zhang, Z., Lin, S. Y., Neel, B. G., and Haimovich, B. (2006) *J. Biol. Chem.* **281,** 1746–1754
23. Choi, C. K., Vicente-Manzanares, M., Zareno, J., Whitmore, L. A., Mogilner, A., and Horwitz, A. R. (2008) *Nat. Cell Biol.* **10,** 1039–1050